CHEMISTRY
AN ASIAN JOURNAL

DOI: 10.1002/asia.200800119

Investigations of the Growth Kinetics of Capped CdSe and CdS Nanocrystals by a Combined Use of Small Angle X-ray Scattering and Other Techniques

Neenu Varghese,[a] Kanishka Biswas,[a, b] and C. N. R. Rao*[a, b]

Dedicated to Professor Ryoji Noyori on the occasion of his 70th birthday

Abstract: The growth of capped CdSe and CdS nanocrystals formed by the reaction of selenium or sulfur with cadmium stearate in toluene solution in the presence of dodecanethiol or trioctylphosphine oxide and tetralin, has been investigated by a variety of techniques to obtain reliable data. Whereas small angle X-ray scattering has provided statistically satisfactory data on the variation of size distribution with time, TEM has been used as a direct probe of the particle size, although with a limited sampling size. UV/Vis and photoluminescence spectroscopies have also provided information about the time evolution of the average diameter (D) of the nanocrystals. By employing all these techniques, we have obtained the $D(t)$ data and fitted then to various growth models. Although certain qualitative observations suggest growth of the nanocrystals to be controlled by diffusion-limited Ostwald ripening, we have found it is necessary to include the surface reaction term in the growth equation. Thus, the growth of CdSe and CdS nanocrystals has contributions from both diffusion and surface reaction, with a D^3+D^2 type behavior, independent of the capping agent.

Keywords: electron microscopy · growth factors · kinetics · nanostructures · small angle X-ray scattering

Introduction

The mechanism for the growth of nanocrystals has attracted significant attention recently in view of its importance, both academically and technologically.[1,2] A popular mechanism employed to explain the growth kinetics of nanocrystals is the diffusion-limited Ostwald ripening process following the Lifshitz-Slyozov-Wagner (LSW) theory.[3,4] Alivisatos and coworkers[5] examined the growth of CdSe and InAs nanocrystals by employing UV/Vis absorption spectroscopy to determine the size of nanocrystals, and the bandwidths in the photoluminescence spectra to determine their size distribution. They observed a focusing and defocusing effect of the size distribution similar to that expected in Ostwald ripening. Qu et al.[6] noted an asymmetric diameter distribution similar to that expected for diffusion-limited Ostwald ripening at the last stage of the growth mechanism in the case of CdSe nanocrystals. Peng and Peng[7,8] examined the growth kinetics of CdSe nanorods by UV/Vis spectroscopy and transmission electron microscopy (TEM), and found the diffusion-controlled model to be valid when the monomer concentration was sufficiently high. Searson and coworkers[9–11] found the growth of ZnO and TiO_2 nanocrystals to follow Ostwald ripening as the dominant mechanism. Our own study of growth kinetics of uncapped ZnO nanorods[12] has shown a diffusion-controlled growth. Based on an in-situ TEM investigation, El-Sayed and coworkers[13] reported a diffusion-controlled growth of small gold nanoclusters.

There are several reports in the literature, in which the growth kinetics of nanocrystals is observed to deviate from the simple diffusion-limited Ostwald ripening model. Seshadri et al.[14] propose the growth of gold nanocrystals to be essentially stochastic, wherein the nucleation and growth steps are well separated. A recent study of the nucleation and growth of gold nanocrystals by small angle X-ray scattering (SAXS) and UV/Vis spectroscopy over a very short time scale suggests a surface reaction-limited growth of nanocrys-

[a] N. Varghese, K. Biswas, Prof. Dr. C. N. R. Rao
Chemistry and Physics of Materials Unit
DST Nanoscience Unit and CSIR Centre of Excellence in Chemistry
Jawaharlal Nehru Centre for Advanced Scientific Research
Jakkur P. O, Bangalore 560064 (India)
Fax: (+91) 80 2208 2760
E-mail: cnrrao@jncasr.ac.in

[b] K. Biswas, Prof. Dr. C. N. R. Rao
Solid State and Structural Chemistry Unit
Indian Institute of Science
Bangalore 560012 (India)

tals in the presence of an alkanoic acid.[15] The slow growth kinetics of gold nanocrystals has been recently reported to follow a sigmoidal growth law rather than Ostwald ripening.[16] Sarma and coworkers[17] reported that the growth kinetics of CdS and ZnS nanocrystals, investigated by SAXS, does not follow the Ostwald-ripening model. These workers also reported that the growth kinetics of the ZnO nanocrystals in the absence of any capping agent, deviates from diffusion-controlled Ostwald ripening.[18,19] These studies, as well as the theoretical studies of Talapin et al.[20] suggested that the growth kinetics of nanocrystals are best explained on the basis of a combined model containing both the diffusion of monomers and the reaction at the surface. Growth kinetics of nanocrystals in the presence of capping agents is controlled by several factors, and signatures of either the diffusion or the surface reaction-controlled regimes are seen. The effect of capping agents on the growth of nanocrystals has been examined by a few workers.[5–8,21–27] For example, the growth kinetics of ZnO nanorods in the presence of poly(vinyl pyrollidone) (PVP) is best explained on the basis of a combined growth model involving both diffusion and surface reaction.[12]

In view of the importance of understanding of the detailed growth mechanism of II-VI semiconductor nanocrystals, we considered it valuable to investigate the growth kinetics of CdSe and CdS nanocrystals over relatively long periods by employing a variety of techniques. Most of the studies of the growth kinetics of CdSe and CdS nanocrystals reported in the literature are based on UV/Vis and photoluminescence (PL) spectroscopies, which are indirect and are strongly affected by the change in the electronic structure of the nanomaterials. We have therefore employed SAXS along with TEM, and UV/Vis and PL spectroscopies for our study of the growth kinetics of CdSe and CdS nanocrystals. Employing such independent techniques is important because of the limitations of each of the techniques. SAXS provides a direct probe to determine the size and shape of nanomaterials, and the sampling size is very much larger than that in TEM measurements. Additionally, SAXS is most suited for an in-situ study of the growth of nanocrystals. We have also obtained the size distribution of the nanocrystals by TEM at different times of growth. Although TEM is the most direct probe to obtain the size, shape, and size distribution of nanostructures, it is not possible to carry out in-situ measurements, especially when the initial nanostructures are small in size.

We have employed a solvothermal reaction between cadmium stearate [$Cd(st)_2$] and Se or S powder, in the presence of dodecanethiol or trioctylphosphine oxide (TOPO) in toluene and a catalytic amount of tetralin.[28,29] We have obtained growth-kinetic data starting with different initial concentrations of $Cd(st)_2$, and report the results of this study in this article. Our study has provided good kinetic data on the growth of CdSe and CdS nanocrystals. The data, however, do not conform to diffusion-limited Ostwald ripening in both cases. The growth mechanism in both CdSe and CdS nanocrystals deviates from the diffusion-limited LSW model, requiring the inclusion of an additional contribution from a surface process.

Results and Discussion

SAXS measurements on the growth of dodecanethiol-capped CdSe nanocrystals were carried out at different initial concentrations of $Cd(st)_2$. Figure 1 a and b shows typical

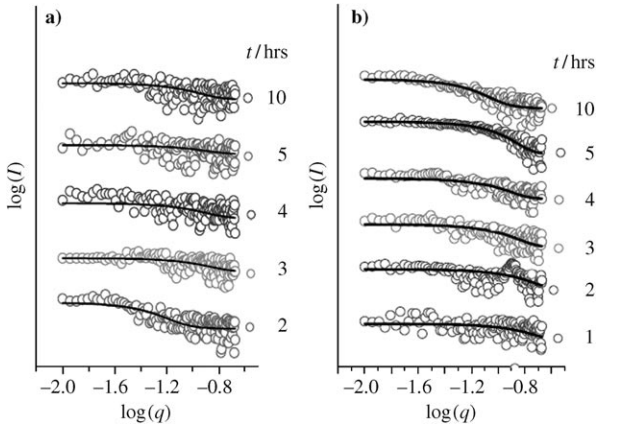

Figure 1. SAXS data for the growth of CdSe nanocrystals prepared from a) 0.05 g (0.07 mmol), and b) 0.2 g (0.29 mmol) of cadmium stearate after different times of the reaction. Solid lines are the spherical model fits to the experimental data.

logarithmic scale plots of intensity versus scattering vector for different times of growth in the case of nanocrystals prepared with 0.05 g (0.07 mmol) and 0.2 g (0.29 mmol) of $Cd(st)_2$, respectively. The changes observed in the SAXS patterns clearly indicate that the nanocrystals grow as a function of time at both concentrations of $Cd(st)_2$ investigated. To estimate the average diameter and diameter distribution of CdSe nanocrystals, we have fitted the experimental SAXS data to the spherical model mentioned in the Experimental Section. The scattering contrast for X-rays is given by the electron-density difference between the particle and the solvent. As CdSe has a higher contrast than the solvent, only the CdSe particles need to be considered for analysis. In the case of a diluted assembly of spherical particles, neglecting particle interaction, the scattering intensity is given by Equation (1)

$$I(q) \propto \int f(R)V(R)^2P(q,R)dR \quad (1)$$

in which $V(R)$ and $P(q, R)$ are the volume and form factor, respectively, of a sphere of radius, R. The form factor of the sphere is given by Equation 2.

$$P(q,R) = \left[\frac{3\{\sin(qR) - qR\cos(qR)\}}{(qR)^3}\right]^2 \quad (2)$$

CHEMISTRY
AN ASIAN JOURNAL

In Equation (2), q is the scattering vector ($q = 4\pi Sin\theta/\lambda$, in which, θ is scattering angle and λ is X-ray wave length), and R, the radius of the sphere. To obtain the particle size distribution, we used the Gaussian distribution, $f(R)$ in Equation (3).

$$f(R) = \frac{1}{\sigma\sqrt{2\pi}} e^{-\left[(R-R_0)^2/2\sigma^2\right]} \quad (3)$$

Least-square refinement yields two parameters, R and σ, in which the latter is the standard deviation. The solid curves in Figure 1 are the sphere-model fits of the experimental SAXS data. The fits with the experimental patterns are quite good, yielding the average diameter, as well as the diameter distributions for different growth times.

We have estimated the diameter, D, of the CdSe nanocrystals after different periods of growth from the SAXS data, and show the time evolution of the diameter distribution in Figure 2a in the case of nanocrystals prepared with 0.2 g (0.29 mmol) of $Cd(st)_2$. Figure 2b represents the corresponding time evolution of the standard deviation of the diameter distribution, σ_D (i.e. half-width of the diameter distribution). The width of the diameter distribution increases up to a certain time, undergoes a sudden drop, and finally reaches a maximum value. We have observed a similar fluctuation in the diameter distribution in the case of CdSe nanocrystals prepared from a lower concentration of $Cd(st)_2$. Such focusing and defocusing of the diameter and length distributions has been noticed earlier in the case of CdSe nanoparticles[5] and of ZnO nanorods.[12] When the monomer concentration gets depleted, arising from the faster growth of the nanocrystals, the smaller nanocrystals start to shrink, while the bigger ones keep growing. The size distribution, therefore, becomes broader (e.g., t = 3 hrs). Dissolution of the small nanocrystals again enriches the monomer concentration in the solution, with the growth of the bigger nanocrystals continuing through the diffusion of the monomer from solution to the nanocrystals surface, giving rise to a focusing of the diameter distribution (e.g., t = 4 to 5 hrs). The focusing and defocusing of the diameter distribution is, thus, dependent on the variation of the monomer concentration in the solution, indicating that the growth of CdSe nanocrystals occurs, at least partly, by diffusion of monomer from the solution to the surface of the nanocrystals.

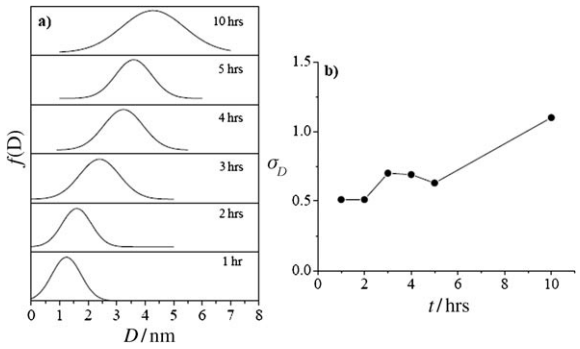

Figure 2. a) Time evolution of diameter distribution of the CdSe nanocrystals prepared from 0.2 g (0.29 mmol) of cadmium stearate and b) the corresponding time evolution of the standard deviation, σ_D, of diameter distribution. The distributions are obtained from the spherical model fits to the experimental SAXS data, recorded after different reaction times (1–10 hrs).

We have carried out TEM measurements at a few points during the growth of the CdSe nanocrystals. Figure 3 shows typical TEM images of CdSe nanocrystals prepared with (0.2 g, 0.29 mmol) of $Cd(st)_2$ after different periods of growth to illustrate how the size of the CdSe nanocrystals increases with increasing growth time. We have estimated the average diameter and the diameter distribution of CdSe nanocrystals at different stages of the growth from the TEM images. Although the TEM data are not statistically as satisfactory as SAXS, the diameter distributions obtained from TEM and SAXS after 3, 4, 5, and 10 h of growth show good agreements.

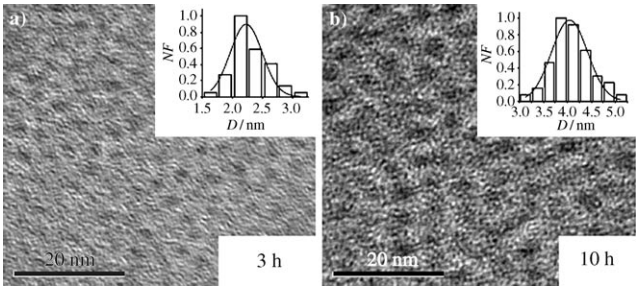

Figure 3. TEM images of CdSe nanocrystals prepared from 0.2 g (0.29 mmol) of cadmium stearate obtained after a) 3 and b) 10 hrs of growth. Insets show the diameter distributions obtained from TEM. NF: normalized frequency.

We have also carried out UV/Vis and PL spectroscopy measurements to obtain additional information on the growth kinetics of CdSe nanocrystals. Figure 4a and b, respectively represent the time evolution of UV/Vis and PL spectra of the CdSe nanocrystals prepared from 0.2 g (0.29 mmol) of $Cd(st)_2$. The UV/Vis spectra show three

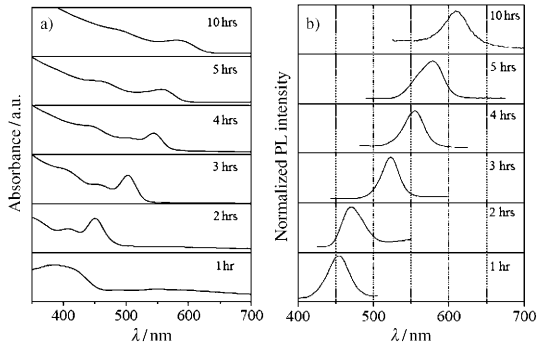

Figure 4. a) UV/Vis spectra and b) photoluminescence spectra of CdSe nanocrystals prepared from 0.2 g (0.29 mmol) of cadmium stearate obtained after different times of growth (1–10 hrs).

clearly resolved bands at approximately 410, 458, and 505 nm after 3 h of the reaction, which is consistent with that reported in the literature.[5,28,30] With increasing reaction time, the absorption bands of CdSe nanocrystals are red-shifted from 400 to 600 nm as the particle size increases. We have calculated the average diameters of the CdSe nanocrystals after different times of the reaction from the UV/Vis spectra following the method described in the Experimental Section.

The PL spectra of CdSe nanocrystals in Figure 4b show clearly resolved band-edge luminescence (e.g., 518 nm band after 3 h of reaction), which is consistent with the literature.[5,6,28,30] The PL band of CdSe nanocrystals is red-shifted from 455 to 615 nm with increasing reaction time. The width of the PL spectra also provides information about the particle-size distribution.[6] The width of the PL band changes with an increase in reaction time similar to the relationship observed for the width of diameter distribution with time (Figure 2). The diameter distributions derived from PL bands are similar to those from SAXS, showing a broadening and narrowing of the PL bandwidth with reaction time.[6] Surprisingly, the PL bands become symmetric (t = 1, 3, 4, and 10 h) and asymmetric (t = 2 and 5 h) during the growth of the particle. The LSW theory of growth predicts an asymmetric size distribution.[2,3] Thus, the PL data reveal that the diffusion-limited reaction contributes to the growth of CdSe nanocrystals.

In Figure 5, we have shown the time evolution of the average diameter obtained from SAXS (filled circles), TEM (open circles) and UV/Vis spectroscopy (open triangles) of the CdSe nanocrystals prepared with two different concentrations of $Cd(st)_2$. The diameters obtained from different techniques are in close agreement. The diameter of the CdSe nanocrystals varies from 1 to 2.1 nm and from 1.3 to 4.4 nm when the starting $Cd(st)_2$ concentrations are 0.07 and 0.29 mmol, respectively. With increasing concentration of $Cd(st)_2$, the diameter of CdSe nanocrystals increases, with higher monomer concentrations favoring the formation of bigger CdSe nanocrystals.

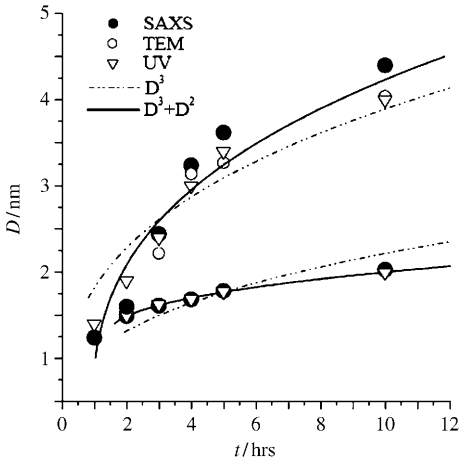

Figure 5. Time evolution of the average diameter (D) of the CdSe nanocrystals obtained from SAXS for different concentrations of cadmium stearate (filled circles). TEM data are shown by open circles. Average diameter calculated from UV/Vis spectra are given by open triangles. Solid curves represent fits of the data to the combined surface- and diffusion-growth model. Dotted curve is the Ostwald ripening-model fit to the experimental data.

Although some qualitative evidence for the diffusion-limited growth of CdSe nanocrystals is provided by the observation of the focusing and defocusing diameter distribution, a better insight is obtained from the time evolution of the average diameter of nanocrystals. If the diffusion-limited Ostwald ripening according to LSW theory[3,4] were the sole contributor for the growth, the rate law would be given by Equation (4)[2]

$$D^3 - D_0^3 = Kt \tag{4}$$

in which D is the average diameter at time t, and D_0, the average initial diameter of the nanocrystals. The rate constant K is given by $K = 8\gamma d V_m^2 C_\infty / 9RT$, with d the diffusion constant at temperature T, V_m, the molar volume, γ, the surface energy, and C_∞, the equilibrium concentration at a flat surface. We have tried to fit the $D(t)$ data of the CdSe nanocrystals obtained from SAXS, TEM, and UV/Vis spectroscopy to the Ostwald-ripening model and found that it was not possible to obtain a good fit of the $D(t)$ data by using Equation (4). A typical fit, using Equation (4), of the $D(t)$ data of the CdSe nanocrystals obtained, is shown in Figure 5 by the broken curve. The fit is not satisfactory with a coefficient of determination, R^2, of 0.33 and 0.58 for 0.07 and 0.29 mmol of $Cd(st)_2$, respectively. The growth process clearly deviates from diffusion-limited Ostwald ripening. We have tried to fit the $D(t)$ data to the surface-limited reaction model ($D^2 \propto t$) or by varying the value of the exponent (n in $D^n \propto t$,), and found that the fit of the data was unsatisfactory to both the surface-reaction model and to a variable-n model.[2] To fit the experimental $D(t)$ data of the CdSe nanocrytals, we have, therefore, used a model which contains both the diffusion-limited and surface-limited growth,[2,12,19] shown in Equation (5)

$$BD^3 + CD^2 + const = t \tag{5}$$

in which, $B = AT/\exp(-E_a/k_BT)$, $A \propto 1/(D_0\gamma V_m^2 C_\infty)$ and $C \propto T/(k_d\gamma V_m^2 C_\infty)$, k_d is the rate constant of surface reaction. The goodness of fits with $R^2 = 0.99$ and 0.97 for the lower and higher concentrations of $Cd(st)_2$, respectively, over the entire range of experimental data by the combined diffusion and surface reaction-control model is shown by the thick solid curve in Figure 5. The observed improvement to the fitting of the data suggests that the growth of the CdSe nanocrystals appears to have contributions from the surface reaction as well.

We have studied the effect of a capping agent on the growth kinetics of CdSe nanocrystals. For this purpose, we have employed trioctylphosphine oxide (TOPO) in place of dodecanethiol keeping the other conditions same at the time of the reaction. We have estimated the diameters and

CHEMISTRY
AN ASIAN JOURNAL

diameter distributions of TOPO-capped CdSe nanocrystals after different times of the reaction by using SAXS, TEM, UV/Vis, and photoluminescence, as was undertaken for the dodecanethiol-capped CdSe nanocrystals. In Figure 6, we show the average diameter of TOPO-capped CdSe nanocrystals obtained from SAXS, TEM, and UV/Vis spectroscopy after different times of the reaction. Diameters obtained from the different techniques show close agreement. The diameter of the CdSe nanocrystals varies from 1.1 to 2.7 nm when the starting $Cd(st)_2$ concentration is 0.29 mmol. In the presence of TOPO, the increase in diameter is somewhat smaller compared to that observed in the dodecanethiol-capped case. We have found the Ostwald ripening model [Eq. (4)] to be unsatisfactory for the data with TOPO as capping agent. Utilising the surface-limited reaction model or by variation of the exponent (n in $D^n \propto t$,), does not provide a good agreement with the experimentally obtained results. We have therefore used the combined model, Equation (5), containing both diffusion-limited and surface-limited growth. The fit is good over the entire range of the data ($R^2 = 0.997$, solid curve in Figure 6). Thus, the growth of the TOPO-capped CdSe also follows the combined diffusion and surface reaction-control model.

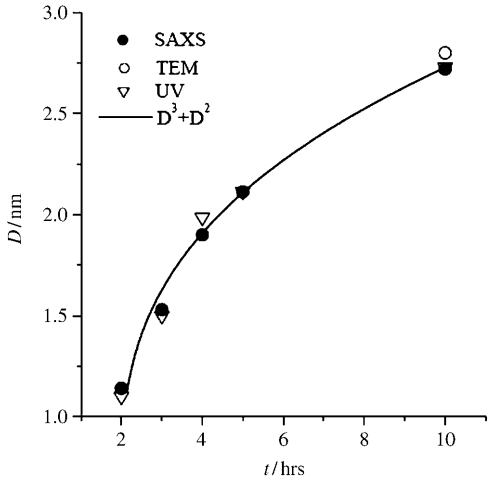

Figure 6. Time evolution of the average diameter (D) of the CdSe nanocrystals obtained from SAXS using TOPO as the capping agent (filled circles). TEM data are shown by open circles. Average diameter calculated from UV/Vis spectra are given by open triangles. Solid curves represent the combined surface and diffusion growth-model fits to the experimental data.

We have carried out studies on the growth kinetics of the dodecanethiol-capped CdS nanocrystals by a combined use of SAXS, TEM, and UV/Vis and photoluminescence spectroscopy. Figure 7 shows typical intensity versus scattering vector plots in the logarithmic scale for different times of growth in the case of CdS nanocrystals prepared with 0.05 g (0.07 mmol) of $Cd(st)_2$. To estimate the average diameter and diameter distribution of CdS nanocrystals, we have fitted the experimental SAXS data to the spherical model. The width of the diameter distribution obtained from SAXS shows the similar focusing and defocusing observed in the case of CdSe nanocrystals. We have also carried out TEM measurements on the CdS nanocrystals at a few points during the growth, and Figure 8 shows typical TEM images of CdS nanocrystals prepared with 0.05 g (0.07 mmol) of $Cd(st)_2$ after different periods of growth. We have estimated the average diameter and the diameter distribution of CdS nanocrystals at different stages of the growth from the TEM images. Although the TEM data are not expected to be as

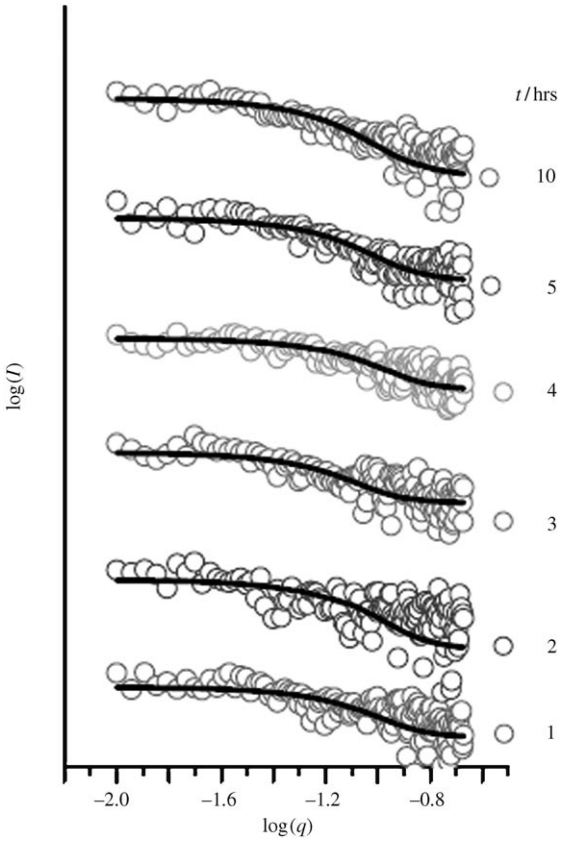

Figure 7. SAXS data for the growth of CdS nanocrystals prepared from a) 0.05 g (0.07 mmol) of cadmium stearate after different times of the reaction. Solid lines are the spherical-model fits to the experimental data.

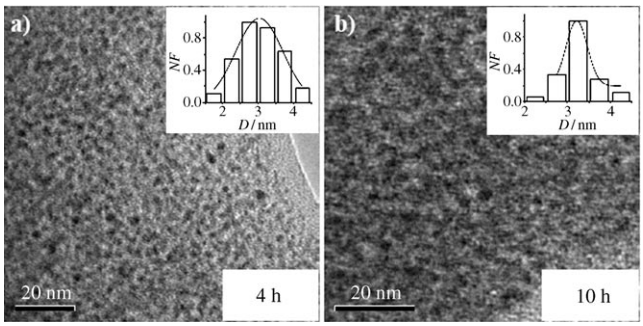

Figure 8. TEM images of CdS nanocrystals prepared from 0.05 g (0.07 mmol) of cadmium stearate obtained after a) 4 and b) 10 hrs of growth. Insets show the diameter distributions obtained from TEM. NF: normalized frequency.

statistically satisfactory as SAXS, the diameter distributions obtained from TEM and SAXS after 4 and 10 h of growth are in good agreement.

Figure 9 represents the time evolution of UV/Vis spectra of the CdS nanocrystals prepared from 0.05 g (0.07 mmol) of $Cd(st)_2$. The UV/Vis spectra show one transition (e.g., 375 nm band after 3 h of the reaction) that is consistent with the literature.[30] With increasing reaction time, the absorption bands of CdS nanocrystals are red-shifted from 360 to 390 nm as the particle size increases. The PL spectra of CdS are not as good as those obtained from CdSe. The band-edge luminescence is obtained to be about 370 nm after 2 h of the reaction.

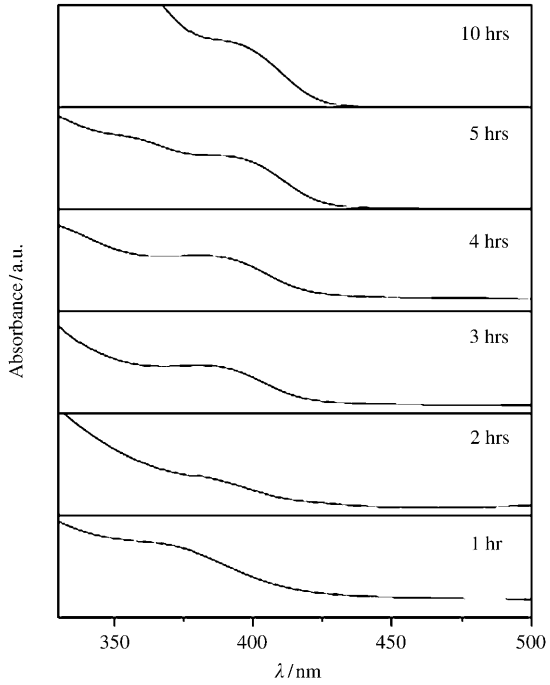

Figure 9. UV/Vis spectra of CdS nanocrystals prepared from 0.05 g (0.07 mmol) of cadmium stearate obtained after different times of growth (1–10 hrs).

Figure 10 shows the plot of the average diameter obtained from SAXS (filled circles), TEM (open circles), and UV/Vis spectroscopy (open triangles) of CdS nanocrystals against time. Diameters obtained from different techniques exhibit close agreement. The diameter of the CdS nanocrystals varies from 2.3 to 3.1 nm when the starting $Cd(st)_2$ concentration is 0.07 mmol. We tried to fit the *D(t)* data to the Ostwald-ripening model [Eq. (4)], yet an unsatisfactory fit was obtained having an R^2 value of only 0.85. A typical fit of the *D(t)* data to Equation (4) of the CdS nanocrystals is shown in Figure 10 by the broken curve. The growth process clearly deviates from the diffusion-limited Ostwald ripening model. We found a good fit of the data only with the combined model, shown in Equation (5), accounting for both diffusion-limited and surface-limited growth. The fit is good over the entire range of the data ($R^2 = 0.99$, solid curve in Figure 10). Thus, the growth of the CdS deviates sufficiently from the diffusion-limited Ostwald-ripening model, and follows a mechanism involving both diffusion-control and surface-reaction control.

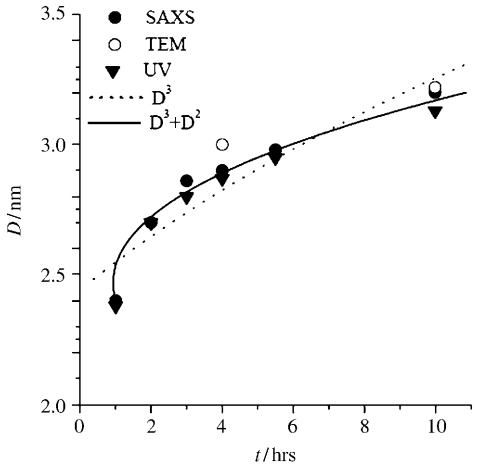

Figure 10. Time evolution of the average diameter (*D*) of the CdS nanocrystals obtained from SAXS for 0.05 g (0.07 mmol) of cadmium stearate (filled circles). TEM data are shown by open circles. Average diameter calculated from UV/Vis spectra are given by solid triangles. Solid curves represent the combined surface and diffusion growth-model fits to the experimental data. Dotted curve is the Ostwald ripening-model fit to the experimental data.

The growth of the nanocrystals mainly occurs by the diffusion of monomers from solution to the nanocrystal surface, or by the reaction at the surface, at which units of the diffusing particles get assimilated into the growing nanocrystals. Diffusion and surface reaction are the limiting cases in the nanocrystal growth. The presence of a capping agent in both cases, gives rise to a barrier to diffusion. The contribution of the surface reaction, therefore, comes into picture. The growth of capped CdSe and CdS nanocrystals clearly occurs through a combination of diffusion and surface-reaction processes.

Conclusions

A systematic study of the growth of capped CdSe and CdS nanocrystals has been carried out by a combined use of SAXS, TEM, UV/Vis, and PL spectroscopies to obtain reliable data on the growth kinetics. The rate of growth was sufficiently slow to follow the kinetics over a long period. Thus, the data represent the kinetics of the growth immediately after the nucleation, which probably occurs within a minute or so. With an increase in the concentration of the starting metal precursor, $Cd(st)_2$, the diameter of the CdSe nanocrystals increases. Focusing and defocusing of the diameter distribution, and the asymmetric nature of the PL band of the nanocrystals, reveal that the diffusion of the monomer contributes towards the growth of the nanocrystals. However, the best fits of the *D(t)* data is found to be a D^3+D^2 model, suggesting that the growth mechanism of capped CdSe and

CdS nanocrystals involves both diffusion and surface reactions. The presence of a capping agent, gives rise to a barrier to diffusion, thereby rendering the contribution of the surface reaction relevant.

Experimental Section

Synthesis

CdSe nanocrystals: To carry out the growth study, CdSe nanocrystals were prepared by the reaction of cadmium stearate and selenium powder in toluene at 250 °C under solvothermal conditions as reported in the literature.[28] The reaction was stopped at different times (1, 2, 3, 4, 5, and 10 h) and the products were analyzed by using TEM and SAXS, and UV/Vis and photoluminescence spectroscopies. In a typical synthesis, cadmium stearate (0.2 g, 0.29 mmol) and selenium powder (0.023 g, 0.29 mmol) were added to toluene (20 mL), followed by the addition of tetralin (30.4 μL) and 1-dodecanethiol (17.4 μL). The reaction mixture was sealed in a teflon-lined autoclave (60% filling fraction) and maintained at 250 °C in a hot air oven. The solid products obtained at different times after the reaction were precipitated with the addition of 2-propanol. The precipitate was collected by centrifugation and redissolved in toluene. To study the effect of the concentration of the reactants on the growth process, we prepared CdSe nanocrystals at a lower concentration of cadmium stearate (0.05 g, 0.07 mmol) keeping the other reaction parameters the same. The samples were taken out after different reaction times (2, 3, 4, 5, and 10 h) for investigation. To study the effect of the capping on the growth process, we prepared CdSe nanocrystals using trioctylphosphine oxide, TOPO, as capping agent (0.0038 g, 0.00 9 mmol) instead of 1-dodecanethiol keeping the other reaction parameters the same. The samples were taken out after different reaction times (2, 3, 4, 5, and 10 h) for investigation.

CdS nanocrystals: To carry out the growth study, CdS nanocrystals were prepared by the reaction of cadmium stearate and sulfur powder in toluene at 250 °C under solvothermal conditions as reported in the literature.[29] The reaction was stopped at different times (1, 2, 3, 4, 5, and 10 h) and the products were analyzed by using TEM and SAXS, and UV/Vis and photoluminescence spectroscopies. In a typical synthesis, cadmium stearate (0.05 g, 0.07 mmol) was dissolved in toluene (20 mL), and sulfur powder (2.4 mg, 0.07 mmol), tetralin (30.4 μL), and 1-dodecanethiol (17.4 μL) were added under stirring. The reaction mixture was sealed in a teflon-lined autoclave (60% filling fraction) and maintained at 250 °C in a hot air oven. The solid products obtained at different times after the reaction, were precipitated with the addition of 2-propanol. The precipitate was collected by centrifugation and redissolved in toluene.

Characterizations

SAXS: The average diameter of the CdSe and CdS nanocrystals could be readily obtained by SAXS[31–33]. We performed SAXS experiments with a Bruker-AXS NanoSTAR instrument modified and optimized for solution scattering. The instrument is equipped with an X-ray tube (Cu K_α radiation, operated at 45 kV/35 mA), cross-coupled Göbel mirrors, three-pinhole collimation, evacuated beam path, and a 2D gas-detector (HI-STAR)[33]. The accessible scattering range of the instrument can be varied by selecting different distances between the sample and the detector of 42.2 cm and 66.2 cm. The modulus of the scattering vector is $q = 4\pi Sin\theta/\lambda$, in which, θ is scattering angle and λ is X-ray wavelength. We recorded the SAXS data in the $q = 0.007$ to 0.21 $Å^{-1}$ range, that is, $2\theta = 0.1$ to 3°. Solutions of the CdSe and CdS nanocrystals in toluene (approximately 0.1 w/v% concentration) obtained after lapse of different reaction times, were used for SAXS measurements. The solutions of nanocrystals were taken in quartz capillaries (diameter of about 2 mm) for the measurements with an exposure time of 20 min in order to obtain good signal-to-noise ratios. A capillary filled with only toluene was used for background correction. The concentration of the nanocrystals was sufficiently low to neglect interparticle-interference effects. The experimental SAXS data were fitted using Bruker-AXS DIFFRAC^{plus} NANOFIT software using a solid-sphere model. The form factor of the spheres used in this software, is that arising from Rayleigh.[34] The assumption of the spherical model was verified by carrying out TEM investigations at several points of the growth process.

TEM: The solid products obtained after different reaction periods, were dissolved in toluene and were taken on holey carbon-coated Cu grids for TEM investigations with a JEOL (JEM3010) microscope operating with an accelerating voltage of 300 kV. The diameter distributions were obtained from the magnified micrograph by using a DigitalMicrograph 3.4 software.

UV/Vis and Photoluminescence: The UV/Vis spectroscopy measurements were performed using a Perkin–Elmer Lambda 900 UV/VIS/NIR spectrophotometer. The nanocrystals were dissolved in toluene, and the solution was used to carry out the UV/Vis measurements. Photoluminescence spectra of these solutions were recorded with a Perkin–Elmer model LS55 luminescence spectrophotometer. The average diameter of the nanocrystals was calculated from the absorption peak position using the sizing curves given in the literature.[35] The sizing curves provided the diameter of CdSe and CdS nanocrystals, which was calculated by using TEM and XRD and the first absorption peak position.

[1] C. N. R. Rao, P. J. Thomas, G. U. Kulkarni, *Nanocrystals: Synthesis Properties and Applications*, Springer, Berlin **2007**.
[2] *Nanomaterials Chemistry: Recent Developments and New Directions* (Eds.: C. N. R. Rao, A. Muller, A. K. Cheetham), Wiley-VCH, Weinheim, **2007**.
[3] I. M. Lifshitz, V. V. Slyozov, *Phys. Chem. Solids* **1961**, *19*, 35–50.
[4] C. Wagner, *Z. Elektrochem.* **1961**, *65*, 581–590.
[5] X. Peng, J. Wickham, A. P. Alivisatos, *J. Am. Chem. Soc.* **1998**, *120*, 5343–5344.
[6] L. Qu, W. W. Yu, X. Peng, *Nano Lett.* **2004**, *4*, 465–469.
[7] Z. A. Peng, X. Peng, *J. Am. Chem. Soc.* **2001**, *123*, 1389–1395.
[8] Z. A. Peng, X. Peng, *J. Am. Chem. Soc.* **2002**, *124*, 3343–3353.
[9] E. M. Wong, J. E. Bonevich, P. C. Searson, *J. Phys. Chem. B* **1998**, *102*, 7770–7775.
[10] Z. Hu, D. J. E. Ramírez, B. E. H. Cervera, G. Oskam, P. C. Searson, *J. Phys. Chem. B* **2005**, *109*, 11209–11214.
[11] G. Oskam, A. Nellore, R. L. Penn, P. C. Searson, *J. Phys. Chem. B* **2003**, *107*, 1734–1738.
[12] K. Biswas, B. Das, C. N. R. Rao, *J. Phys. Chem. B* **2008**, *112*, 2404–2411.
[13] M. B. Mohamed, Z. L. Wang, M. A. El-Sayed, *J. Phys. Chem. A* **1999**, *103*, 10255–10259.
[14] R. Seshadri, G. N. Subbanna, V. Vijayakrishnan, G. U. Kulkarni, G. Ananthakrishna, C. N. R. Rao, *J. Phys. Chem.* **1995**, *99*, 5639–5644.
[15] B. Abecassis, F. Testard, O. Spalla, P. Barboux, *Nano Lett.* **2007**, *7*, 1723–1727.
[16] K. Biswas, N. Varghese, C. N. R. Rao, *Small* **2008**, *4*, 649–655.
[17] R. Viswanatha, S. Sapra, H. Amenitsch, B. Sartori, D. D. Sarma, *J. Nanosci. Nanotechnol.* **2007**, *7*, 1726–1729.
[18] R. Viswanatha, H. Amenitsch, D. D. Sarma, *J. Am. Chem. Soc.* **2007**, *129*, 4470–4475.
[19] R. Viswanatha, P. K. Santra, C. Dasgupta, D. D. Sarma, *Phys. Rev. Lett.* **2007**, *98*, 255501(1–4).
[20] D. V. Talapin, A. L. Rogach, M. Haase, H. Weller, *J. Phys. Chem. B* **2001**, *105*, 12278–12285.
[21] R. Viswanatha, D. D. Sarma, *Chem. Eur. J.* **2006**, *12*, 180–186.
[22] N. S. Pesika, Z. Hu, K. J. Stebe, P. C. Searson, *J. Phys. Chem. B* **2002**, *106*, 6985–6990.
[23] C. R. Bullen, P. Mulvaney, *Nano Lett.* **2004**, *4*, 2303–2307.
[24] W. W. Yu, X. Peng, *Angew. Chem.* **2002**, *114*, 2474–2477; *Angew. Chem. Int. Ed.* **2002**, *41*, 2368–2371.
[25] L. Qu, X. Peng, *J. Am. Chem. Soc.* **2002**, *124*, 2049–2055.
[26] Q. Dai, D. Li, H. Chen, S. Kan, H. Li, S. Gao, Y. Hou, B. Liu, G. Zou, *J. Phys. Chem. B* **2006**, *110*, 16508–16513.
[27] E. M. Wong, P. G. Hoertz, C. J. Liang, B. Shi, G. J. Meyer, P. C. Searson, *Langmuir* **2001**, *17*, 8362–8367.

[28] U. K. Gautam, M. Rajamathi, F. Meldrum, P. Morgan, R. Seshadri, *Chem. Commun.* **2001**, 629–630.
[29] U. K. Gautam, R. Seshadri, C. N. R. Rao, *Chem. Phys. Lett.* **2003**, *375*, 560–564.
[30] C. B. Murray, D. J. Norrish M. G. Bawendi, *J. Am. Chem. Soc.* **1993**, *115*, 8706–8715.
[31] J. S. Pedersen, *Adv. Colloid Interface Sci.* **1997**, *70*, 171–210.
[32] J. S. Pedersen in *Neutrons, X-rays and Light: Scattering Methods Applied to Soft Condensed Matter* (Eds.: P. Lindner, T. Zemb), North-Holland, New York, **2002**, pp. 391–420.
[33] J. S. Pedersen, *J. Appl. Crystallogr.* **2004**, *37*, 369–380.
[34] L. Rayleigh, *Proc. R. Soc. London Ser. A* **1910**, *84*, 25–46.
[35] W. W. Yu, L. Qu, W. Guo, X. Peng, *Chem. Mater.* **2003**, *15*, 2854–2860.

Received: March 23, 2008
Published online: July 21, 2008

